



# Selective reduction of CO to acetaldehyde with CuAg electrocatalysts

Lei Wang<sup>a</sup>, Drew C. Higgins<sup>a,b,c</sup>, Yongfei Ji<sup>a</sup>, Carlos G. Morales-Guio<sup>a</sup>, Karen Chan<sup>b,d</sup>, Christopher Hahn<sup>b,1</sup>, and Thomas F. Jaramillo<sup>a,b,1</sup>

<sup>a</sup>SUNCAT Center for Interface Science and Catalysis, Department of Chemical Engineering, Stanford University, CA 94305; <sup>b</sup>SUNCAT Center for Interface Science and Catalysis, SLAC National Accelerator Laboratory, Menlo Park, CA 94025; <sup>c</sup>Department of Chemical Engineering, McMaster University, Hamilton, ON L8S 4L8, Canada; and <sup>d</sup>CatTheory Center, Department of Physics, Technical University of Denmark, 2800 Kongens Lyngby, Denmark

Edited by Richard Eisenberg, University of Rochester, Rochester, NY, and approved December 17, 2019 (received for review May 16, 2019)

**Electrochemical CO reduction can serve as a sequential step in the transformation of CO<sub>2</sub> into multicarbon fuels and chemicals. In this study, we provide insights on how to steer selectivity for CO reduction almost exclusively toward a single multicarbon oxygenate by carefully controlling the catalyst composition and its surrounding reaction conditions. Under alkaline reaction conditions, we demonstrate that planar CuAg electrodes can reduce CO to acetaldehyde with over 50% Faradaic efficiency and over 90% selectivity on a carbon basis at a modest electrode potential of  $-0.536$  V vs. the reversible hydrogen electrode. The Faradaic efficiency to acetaldehyde was further enhanced to 70% by increasing the roughness factor of the CuAg electrode. Density functional theory calculations indicate that Ag ad-atoms on Cu weaken the binding energy of the reduced acetaldehyde intermediate and inhibit its further reduction to ethanol, demonstrating that the improved selectivity to acetaldehyde is due to the electronic effect from Ag incorporation. These findings will aid in the design of catalysts that are able to guide complex reaction networks and achieve high selectivity for the desired product.**

electrocatalysis | CO<sub>2</sub> reduction | CO reduction | bimetallics | heterogeneous catalysis

Electrochemical CO<sub>2</sub> reduction (CO<sub>2</sub>R) is a promising approach to store renewable energy in the form of energy-dense fuels, or for the sustainable synthesis of feedstock chemicals (1–3). Copper (Cu) is currently the only electrode material that has shown significant CO<sub>2</sub>R activity toward multicarbon fuels and chemicals, albeit with a widely divergent selectivity toward over 16 different products (4–6). Previous studies on Cu electrodes have shown that CO reduction is the rate-limiting step in the transformation of CO<sub>2</sub> to further reduced ( $>2e^-$ ) products (4, 6–11). In addition to providing important mechanistic insights for CO<sub>2</sub>R, direct electrochemical CO reduction (COR) can also serve as a sequential route for reducing CO<sub>2</sub> into multicarbon products when utilized in tandem with existing technologies that can efficiently generate CO from CO<sub>2</sub> (11–13). Thus, there are motivations to understand how to guide COR selectivity to the desired products.

A number of strategies have been developed to address the challenge of steering CO<sub>2</sub>R/COR selectivity, by modifying either the intrinsic or extrinsic properties of the electrocatalytic system (14). Examples of successfully controlling intrinsic properties to guide selectivity include modifying the electrocatalyst surface structure (8, 9, 15–19), composition (20–33), particle size (34–36), and roughness factor (37–39). Similarly, researchers have demonstrated that extrinsic factors such as the electrode potential (11, 39), electrolyte pH (11, 37, 38, 40–43), electrolyte cation identity and concentration (44–46), and molecular additives (47–50) significantly influence reactivity for CO<sub>2</sub>R/COR. Although all of these studies have provided tremendous insights on how to guide selectivity to broad product groups such as C<sub>2+</sub> oxygenates and hydrocarbons, controlling the reaction selectivity toward a specific product is still a major fundamental challenge.

In this work, we leveraged insights from the aforementioned strategies that control the intrinsic and extrinsic properties of electrocatalytic systems, with the aim of steering the selectivity of COR toward a single C<sub>2+</sub> oxygenate. To modify the intrinsic electrocatalytic properties of Cu electrodes, we implemented an Ag galvanic exchange process as previous research indicated that CuAg bimetallic electrocatalysts enhance selectivity toward C<sub>2+</sub> oxygenates by suppressing the competing hydrogen evolution reaction (HER) (22, 28). In addition, alkaline pH conditions were used for COR based on previous studies that show the energy efficiency and selectivity to C<sub>2+</sub> oxygenates can be improved by governing this extrinsic property around the electrocatalyst (11, 51, 52). As hypothesized, we found that the combined approach of directing the intrinsic and extrinsic properties leads to an efficient electrocatalytic system that exhibits a Faradaic efficiency of  $\sim 50\%$  for COR to acetaldehyde, with hydrogen as the only other major product. Remarkably, over 90% of the CO reacted goes to the formation of acetaldehyde. Density functional theory (DFT) calculations explain the high selectivity to acetaldehyde, as the Ag ad-atoms on Cu surface lower the intrinsic activity for acetaldehyde reduction by introducing electronic effects that weaken the binding energy of its key reduction intermediate. The fundamental insights from this work provide general design strategies that can be utilized for the discovery and development of efficient electrocatalytic systems.

## Results and Discussion

Although metallic Ag and Cu are thermodynamically immiscible at room temperature, previous work has demonstrated that CuAg surface alloys with dilute Ag content can be formed by galvanic exchange of Cu with Ag using an Ag ion precursor solution (22). It has been shown that the selectivity of CO<sub>2</sub>R to multicarbon products observed over Cu-based alloys increases concomitantly with the surface composition of Cu, suggesting

This paper results from the Arthur M. Sackler Colloquium of the National Academy of Sciences, “Status and Challenges in Decarbonizing our Energy Landscape,” held October 10–12, 2018, at the Arnold and Mabel Beckman Center of the National Academies of Sciences and Engineering in Irvine, CA. NAS colloquia began in 1991 and have been published in PNAS since 1995. From February 2001 through May 2019 colloquia were supported by a generous gift from The Dame Jillian and Dr. Arthur M. Sackler Foundation for the Arts, Sciences, & Humanities, in memory of Dame Sackler’s husband, Arthur M. Sackler. The complete program and video recordings of most presentations are available on the NAS website at <http://www.nasonline.org/decarbonizing>.

Author contributions: L.W., D.C.H., K.C., C.H., and T.F.J. designed research; L.W., D.C.H., Y.J., and C.G.M.-G. performed research; L.W., D.C.H., Y.J., and C.G.M.-G. analyzed data; and L.W., K.C., C.H., and T.F.J. wrote the paper.

The authors declare no competing interest.

This article is a PNAS Direct Submission.

Published under the PNAS license.

<sup>1</sup>To whom correspondence may be addressed. Email: [chahn@slac.stanford.edu](mailto:chahn@slac.stanford.edu) or [jaramillo@stanford.edu](mailto:jaramillo@stanford.edu).

This article contains supporting information online at <https://www.pnas.org/lookup/suppl/doi:10.1073/pnas.1821683117/-DCSupplemental>.

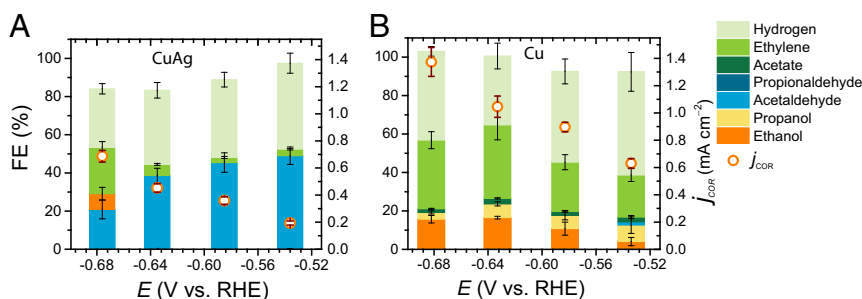


**Fig. 1.** COR on CuAg (A) and Cu (B) (11) electrodes under the same reaction conditions: 0.1 M KOH saturated with 1 atm CO at ambient temperature. Faradaic efficiencies (FE) and geometric current densities for COR ( $j_{\text{COR}}$ ) are shown as a function of the electrode potential. The error bars represent one SD of the results from three independent samples.

that neighboring Cu atomic ensembles are required for efficient C–C coupling (53). Therefore, a low Ag surface content is preferred in order to maintain a surface rich with Cu active sites. Inspired by these previous studies, CuAg electrodes were prepared by immersing prepolished polycrystalline Cu foils into a dilute AgNO<sub>3</sub> solution. At the surface, a relatively high Cu:Ag atomic ratio of about 7:1 was measured for these electrodes as measured by X-ray photoelectron spectroscopy (SI Appendix, Fig. S1).

The product distributions for the CuAg electrodes indicate that acetaldehyde is formed in significant quantities at all electrochemical potentials (Fig. 1A). The highest selectivity toward acetaldehyde is observed at  $-0.536$  V vs. the reversible hydrogen electrode (RHE), with a Faradaic efficiency of *ca.* 50% that accounts for  $\sim 90\%$  of the total CO reduction partial current. Comparing the COR testing results for CuAg versus Cu (Fig. 1 and SI Appendix, Fig. S2), CuAg clearly has a higher selectivity to a single liquid product acetaldehyde, in contrast to pure Cu which forms seven different products at this potential (11), including five different liquid phase species and another two different gas phase products. While the overall selectivity for all COR products remains consistently  $\sim 50\%$  for CuAg within the range of electrode potentials used for testing, there are clearly potential-dependent changes in the product distribution. For example, at more negative electrode potentials, the selectivity toward acetaldehyde decreases concomitantly with an increase in selectivity toward ethylene and eventually ethanol. At  $-0.676$  V vs. RHE, ethanol appears at the expense of acetaldehyde formation (SI Appendix, Fig. S2), supporting the suggestion that acetaldehyde is a precursor to ethanol (11, 54, 55). In contrast, selectivity to ethylene increases at more negative electrode potentials, with Tafel analysis clearly demonstrating that the electrode potential has a stronger impact on activity toward ethylene in comparison to acetaldehyde (SI Appendix, Fig. S2). This difference in the activity dependence on electrode potential indicates that acetaldehyde and ethylene may go through different pathways after CO dimerization, which is consistent with previous theoretical work focused on understanding mechanisms of C<sub>2</sub> product formation (56). Previous studies have shown that cascading homogeneous reactions can influence the CO<sub>2</sub>R/COR product distribution (55, 57). Control <sup>1</sup>H NMR experiments indicate that Cannizzaro-type disproportionation is not a significant homogeneous reaction pathway in 0.1 M KOH (SI Appendix, Fig. S3), suggesting that ethanol formation is likely an electrochemical process under the conditions we used for COR experiments. Instead, these <sup>1</sup>H NMR experiments support a previous conclusion that acetaldehyde can be polymerized by homogeneous reactions in alkaline conditions (55, 58), influencing product quantification for COR. Notably, these reactions appear to be reversible as acetaldehyde can be recovered by simply neutralizing the electrolyte with 0.1 M HCl (SI Appendix, Fig. S3). The suppressed HER activity on CuAg compared to pure Cu (SI Appendix, Figs. S2B and

S4) can be attributed to the presence of Ag atoms at or near the electrode surface, which likely will result in a lower \*H surface coverage under reaction conditions (22, 28). The decrease in overall COR activity (SI Appendix, Fig. S2B) is likely due to Ag galvanic exchange occurring mainly on the stepped and under-coordinated Cu surface sites which are the most intrinsically active sites for COR (15, 17). To further explore the influence of the catalyst composition on reactivity, we used a previously implemented physical vapor deposition method to prepare a broad range of CuAg thin-film compositions with interphase miscibility (SI Appendix, Fig. S5) (28). Unlike previous CO<sub>2</sub>R studies that show a clear dependence of the partial activities on the CuAg composition (22, 26, 28, 29, 31–33), similar activities and selectivities were observed for almost all of the bimetallic thin films (SI Appendix, Fig. S6). This result suggests that the types and proportions of surface active sites are similar for all of these catalysts under alkaline COR conditions, leading to the hypothesis that the surfaces restructure into analogous ensembles during electrolysis. Surface-sensitive *operando* probes could provide further evidence for surface restructuring and guide the future design of new catalysts.

To determine why CuAg is selective for COR to acetaldehyde, we conducted acetaldehyde reduction experiments to compare the activities of Cu and CuAg for producing ethanol (SI Appendix, Fig. S7). The results demonstrate that CuAg is significantly less active than Cu for acetaldehyde reduction, explaining its high selectivity for acetaldehyde. To rationalize the suppression in acetaldehyde reduction, the binding energy of the key reaction intermediate, CH<sub>3</sub>CH<sub>2</sub>O\*, was examined using DFT. The edge sites were calculated to be the most favorable sites for Ag doping (SI Appendix, Fig. S8). Based on our previous study, Ag doping reduces the H\* binding energy of Cu, corroborating

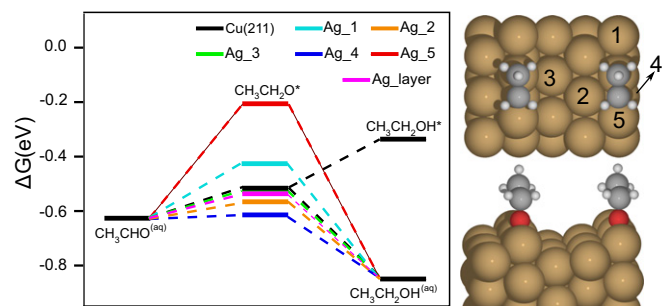


**Fig. 2.** Free energy diagram (Left) for CH<sub>3</sub>CHO\* reduction to ethanol on the Cu(211) surface with Ag doped at different sites. The free energy of CH<sub>3</sub>CHO\* on the pristine Cu(211) surface is taken as an energy reference. (Right) The adsorption structure of CH<sub>3</sub>CH<sub>2</sub>O\* is shown from the top and side view. Ag<sub>n</sub> denotes when Cu(n) on the surface is replaced by Ag. Ag<sub>layer</sub> means the subsurface layer of Cu is replaced by Ag.

the suppression in hydrogen production that is observed experimentally (*SI Appendix, Fig. S2*) (28). Similarly, the most stable adsorption sites of  $\text{CH}_3\text{CH}_2\text{O}$  on the surface are calculated to be the edge sites, as shown in the free energy diagram in Fig. 2. This diagram shows that the potential limiting step for the reduction of  $\text{CH}_3\text{CHO}(\text{aq})$  is the first proton and electron transfer step to form  $\text{CH}_3\text{CH}_2\text{O}^*$ . As the edge Cu (site 1) is replaced by Ag, the binding energy of  $\text{CH}_3\text{CH}_2\text{O}^*$  is weakened by 0.09 eV; when the Cu atom closest to the adsorption site (site 5) is replaced by Ag, the binding of  $\text{CH}_3\text{CH}_2\text{O}^*$  is weakened by 0.31 eV. In both cases there is a substantially higher thermodynamic energy barrier for the conversion of  $\text{CH}_3\text{CHO}^*$  to  $\text{CH}_3\text{CH}_2\text{OH}(\text{aq})$ . Thus, Ag incorporation into Cu mitigates acetaldehyde reduction, thus greatly improving its rate of production, corroborating the experimental results. However, this improvement in product selectivity comes at the cost of decreased overall COR activity, since the Cu edge sites are the most intrinsically active for COR (15). Taken together, the results suggest that manipulating the binding energy of COR reaction intermediates by controlling the catalyst composition is a viable strategy to improve the selectivity for COR toward valuable products. To fully rationalize the high COR selectivity to acetaldehyde on CuAg it will also be important to understand how Ag influences the bifurcation between the acetaldehyde/ethanol and ethylene pathways. Although a number of DFT studies have led to hypotheses on reaction mechanisms (59–62), a putative intermediate common to the bifurcation point between these pathways is yet to be determined either theoretically or experimentally. Identifying a putative intermediate will aid in the understanding of how to control  $\text{CO}_2\text{R}/\text{COR}$  selectivity to a single multicarbon product, such as CuAg for COR.

With the above knowledge in hand, we then aimed to explore the impacts of the electrode surface area on COR selectivity. It has been previously demonstrated that the electrode roughness factor can steer COR selectivity toward multicarbon oxygenates on pure Cu catalysts by suppressing the competing HER (63). To test whether this surface area effect can further enhance the selectivity to acetaldehyde for the CuAg system, a porous CuAg nanoflower electrode (CuAg-NF) was prepared and evaluated for COR similarly. Although the trends in normalized current densities indicate that there are some uncertainties in attempting to translate Ag galvanic exchange technique from the planar morphology to the NF morphology (*SI Appendix, Fig. S9*), we nevertheless observed substantial enhancement in both reaction rate and selectivity to acetaldehyde (Fig. 3). The Faradaic efficiency for acetaldehyde production on the CuAg-NF electrode reached 70% with an overall COR reaction rate three times greater than that of the planar system at an applied potential of only  $-0.33$  V vs. RHE, representing a  $\sim 0.2$  V improvement in overpotential based on the geometric current density. Thus, these results further validate the concept that high electrode surface areas can improve selectivity, not just reaction rates, a

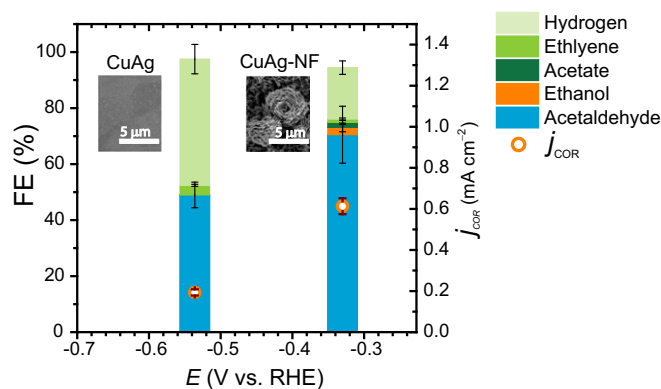


**Fig. 3.** Comparison between COR on planar (CuAg) and porous (CuAg-NF) electrodes under the same reaction conditions: 0.1 M KOH saturated with 1 atm CO at ambient temperature. Faradaic efficiencies (FE) and geometric current densities for COR ( $j_{\text{COR}}$ ) are shown as a function of the electrode potential.

principle that can likely be extended further to other catalyst materials.

## Conclusion

In summary, CuAg bimetallic electrodes have been investigated for CO reduction under alkaline conditions. Unprecedented selectivity to acetaldehyde was obtained at low overpotentials on planar CuAg electrodes. The selectivity and activity to acetaldehyde was further improved by increasing the CuAg electrode surface area. DFT calculations demonstrate that the Ag ad-atoms can tune the surface binding energy of reduced aldehyde intermediates, resulting in a suppression of acetaldehyde reduction to ethanol. This study emphasizes how deliberate modification to the catalyst surface and reaction conditions can greatly improve product selectivity, providing design principles that can be extended to other catalysts and related electrocatalytic reactions.

**Data Availability.** Electrochemical data and other physical characterization data used to produce the results in this paper are provided in *SI Appendix, Figs. S1–S9* and *Table S1*.

**ACKNOWLEDGMENTS.** This material is based upon work performed by the Joint Center for Artificial Photosynthesis, a Department of Energy (DOE) Energy Innovation Hub, supported through the Office of Science of the US DOE under Award DE-SC0004993. Part of this work was performed at the Stanford Nano Shared Facilities, supported by the National Science Foundation, under Award ECCS-1542152. We thank the Stanford NMR Facility. L.W. and Y.J. thank the Knut Alice Wallenberg Foundation for financial support. C.G.M.-G. gratefully acknowledges support from the Swiss National Science Foundation (Grant P400P2\_180767).

- M. Jouny, W. W. Luc, F. Jiao, A general techno-economic analysis of  $\text{CO}_2$  electrolysis systems. *Ind. Eng. Chem. Res.* **57**, 2165–2177 (2018).
- Z. W. She *et al.*, Combining theory and experiment in electrocatalysis: Insights into materials design. *Science* **355**, eaad4998 (2017).
- M. Gattrell, N. Gupta, A. Co, Electrochemical reduction of  $\text{CO}_2$  to hydrocarbons to store renewable electrical energy and upgrade biogas. *Energy Convers. Manage.* **48**, 1255–1265 (2007).
- K. P. Kuhl *et al.*, Electrocatalytic conversion of carbon dioxide to methane and methanol on transition metal surfaces. *J. Am. Chem. Soc.* **136**, 14107–14113 (2014).
- H. Noda *et al.*, Electrochemical reduction of carbon dioxide at various metal electrodes in aqueous potassium hydrogen carbonate solution. *Bull. Chem. Soc. Jpn.* **63**, 2459–2462 (1990).
- Y. Hori, K. Kikuchi, S. Suzuki, Production of CO and  $\text{CH}_4$  in electrochemical reduction of  $\text{CO}_2$  at metal electrodes in aqueous hydrogencarbonate solution. *Chem. Lett.* **11**, 1695–1698 (1985).
- E. Pérez-Gallent, M. C. Figueiredo, F. Calle-Vallejo, M. T. M. Koper, Spectroscopic observation of a hydrogenated CO dimer intermediate during CO reduction on Cu(100) electrodes. *Angew. Chem. Int. Ed. Engl.* **56**, 3621–3624 (2017).
- F. Calle-Vallejo, M. T. M. Koper, Theoretical considerations on the electroreduction of CO to  $\text{C}_2$  species on Cu(100) electrodes. *Angew. Chem. Int. Ed. Engl.* **52**, 7282–7285 (2013).
- Y. Hori, I. Takahashi, O. Koga, N. Hoshi, Selective formation of  $\text{C}_2$  compounds from electrochemical reduction of  $\text{CO}_2$  at a series of copper single crystal electrodes. *J. Phys. Chem. B* **106**, 15–17 (2002).
- A. Peterson, J. Nørskov, Activity descriptors for  $\text{CO}_2$  electroreduction to methane on transition metal catalysts. *J. Phys. Chem. Lett.* **3**, 251–258 (2012).
- L. Wang *et al.*, Electrochemical carbon monoxide reduction on polycrystalline copper: Effects of potential, pressure and pH on selectivity towards multi-carbon and oxygenated products. *ACS Catal.* **8**, 7445–7454 (2018).
- C. Mittal, C. Hadsbjerg, P. Blennow, Small-scale CO from  $\text{CO}_2$  using electrolysis. *Chem. Eng. World* **52**, 44–46 (2017).
- D. C. Higgins, C. Hahn, C. Xiang, T. F. Jaramillo, A. Z. Weber, Gas-diffusion electrodes for carbon dioxide reduction: A new paradigm. *ACS Energy Lett.* **4**, 317–324 (2018).
- A. Vojvodic, J. K. Nørskov, New design paradigm for heterogeneous catalysts. *Natl. Sci. Rev.* **2**, 140–149 (2015).
- X. Liu *et al.*, Understanding trends in electrochemical carbon dioxide reduction rates. *Nat. Commun.* **8**, 15438 (2017).

16. K. J. P. Schouten, E. Pérez Gallent, M. T. M. Koper, Structure sensitivity of the electrochemical reduction of carbon monoxide on copper single crystals. *ACS Catal.* **3**, 1292–1295 (2013).
17. C. Hahn *et al.*, Engineering Cu surfaces for the electrocatalytic conversion of CO<sub>2</sub>: Controlling selectivity toward oxygenates and hydrocarbons. *Proc. Natl. Acad. Sci. U.S.A.* **114**, 5918–5923 (2017).
18. K. J. P. Schouten, Z. Qin, E. Pérez Gallent, M. T. M. Koper, Two pathways for the formation of ethylene in CO reduction on single-crystal copper electrodes. *J. Am. Chem. Soc.* **134**, 9864–9867 (2012).
19. Z. Weng *et al.*, Self-cleaning catalyst electrodes for stabilized CO<sub>2</sub> reduction to hydrocarbons. *Angew. Chem. Int. Ed. Engl.* **56**, 13135–13139 (2017).
20. J. He, K. E. Dettelbach, A. Huang, C. P. Berlinguette, Brass and bronze as effective CO<sub>2</sub> reduction electrocatalysts. *Angew. Chem. Int. Ed. Engl.* **56**, 16579–16582 (2017).
21. D. Ren, B. S. H. Ang, B. S. Yeo, Tuning the selectivity of carbon dioxide electroreduction toward ethanol on oxide-derived Cu<sub>x</sub>Zn catalysts. *ACS Catal.* **6**, 8239–8247 (2016).
22. E. L. Clark, C. Hahn, T. F. Jaramillo, A. T. Bell, Electrochemical CO<sub>2</sub> reduction over compressively strained CuAg surface alloys with enhanced multi-carbon oxygenate selectivity. *J. Am. Chem. Soc.* **139**, 15848–15857 (2017).
23. D. A. Torelli *et al.*, Nickel-gallium-catalyzed electrochemical reduction of CO<sub>2</sub> to highly reduced products at low overpotentials. *ACS Catal.* **6**, 2100–2104 (2016).
24. S. Rasul *et al.*, A highly selective copper-indium bimetallic electrocatalyst for the electrochemical reduction of aqueous CO<sub>2</sub> to CO. *Angew. Chem. Int. Ed. Engl.* **54**, 2146–2150 (2015).
25. M. Li *et al.*, Mesoporous palladium-copper bimetallic electrodes for selective electrocatalytic reduction of aqueous CO<sub>2</sub> to CO. *J. Mater. Chem. A Mater. Energy Sustain.* **4**, 4776–4782 (2016).
26. C. W. Lee *et al.*, Defining a materials database for the design of copper binary alloy catalysts for electrochemical CO<sub>2</sub> conversion. *Adv. Mater.* **30**, e1704717 (2018).
27. S. Sarfraz, A. T. Garcia-Esparza, A. Jedidi, L. Cavallo, K. Takahashi, Cu-Sn bimetallic catalyst for selective aqueous electroreduction of CO<sub>2</sub> to CO. *ACS Catal.* **6**, 2842–2851 (2016).
28. D. Higgins *et al.*, Guiding electrochemical carbon dioxide reduction toward carbonyls using copper silver thin films with interphase miscibility. *ACS Energy Lett.* **3**, 2947–2955 (2018).
29. T. T. H. Hoang *et al.*, Nanoporous copper-silver alloys by additive-controlled electrodeposition for the selective electroreduction of CO<sub>2</sub> to ethylene and ethanol. *J. Am. Chem. Soc.* **140**, 5791–5797 (2018).
30. C. Hahn *et al.*, Synthesis of thin film AuPd alloys and their investigation for electrocatalytic CO<sub>2</sub> reduction. *J. Mater. Chem. A Mater. Energy Sustain.* **3**, 20185–20194 (2015).
31. Y. Wang *et al.*, CO<sub>2</sub> reduction to acetate in mixtures of ultrasmall (Cu)<sub>n</sub> (Ag)<sub>m</sub> bimetallic nanoparticles. *Proc. Natl. Acad. Sci. U.S.A.* **115**, 278–283 (2018).
32. Z. Chang, S. Huo, J. He, J. Fang, Facile synthesis of Cu–Ag bimetallic electrocatalyst with prior C<sub>2</sub> products at lower overpotential for CO<sub>2</sub> electrochemical reduction. *Surf. Interfaces* **6**, 116–121 (2017).
33. J. Choi *et al.*, Electrochemical CO<sub>2</sub> reduction to CO on dendritic Ag–Cu electrocatalysts prepared by electrodeposition. *Chem. Eng. J.* **299**, 37–44 (2016).
34. D. Gao *et al.*, Size-dependent electrocatalytic reduction of CO<sub>2</sub> over Pd nanoparticles. *J. Am. Chem. Soc.* **137**, 4288–4291 (2015).
35. R. Reske, H. Mistry, F. Beharfarid, B. Roldan Cuenya, P. Strasser, Particle size effects in the catalytic electroreduction of CO<sub>2</sub> on Cu nanoparticles. *J. Am. Chem. Soc.* **136**, 6978–6986 (2014).
36. M. Liu *et al.*, Enhanced electrocatalytic CO<sub>2</sub> reduction via field-induced reagent concentration. *Nature* **537**, 382–386 (2016).
37. Y. Yoon, A. S. Hall, Y. Surendranath, Tuning of silver catalyst mesostructure promotes selective carbon dioxide conversion into fuels. *Angew. Chem. Int. Ed. Engl.* **55**, 15282–15286 (2016).
38. M. Ma, K. Djanashvili, W. A. Smith, Controllable hydrocarbon formation from the electrochemical reduction of CO<sub>2</sub> over Cu nanowire arrays. *Angew. Chem. Int. Ed. Engl.* **55**, 6680–6684 (2016).
39. D. Ren, J. Fong, B. S. Yeo, The effects of currents and potentials on the selectivities of copper toward carbon dioxide electroreduction. *Nat. Commun.* **9**, 925 (2018).
40. F. S. Roberts, K. P. Kuhl, A. Nilsson, Electroreduction of carbon monoxide over a copper nanocube catalyst: Surface structure and pH dependence on selectivity. *ChemCatChem* **8**, 1119–1124 (2016).
41. X. Liu *et al.*, pH effects on the electrochemical reduction of CO<sub>2</sub> towards C<sub>2</sub> products on stepped copper. *Nat. Commun.* **10**, 32 (2019).
42. C. Dinh *et al.*, Sustained high-selectivity CO<sub>2</sub> electroreduction to ethylene via hydroxide-mediated catalysis at an abrupt reaction interface. *Science* **787**, 783–787 (2018).
43. S. Ma *et al.*, One-step electrosynthesis of ethylene and ethanol from CO<sub>2</sub> in an alkaline electrolyzer. *J. Power Sources* **301**, 219–228 (2015).
44. A. Murata, Y. Hori, Product selectivity affected by cationic species in electrochemical reduction of CO<sub>2</sub> and CO at a Cu electrode. *Bull. Chem. Soc. Jpn.* **64**, 123–127 (1991).
45. J. Resasco *et al.*, Promoter effects of alkali metal cations on the electrochemical reduction of carbon dioxide. *J. Am. Chem. Soc.* **139**, 11277–11287 (2017).
46. M. R. Thorson, K. I. Siil, P. J. A. Kenis, Effect of cations on the electrochemical conversion of CO<sub>2</sub> to CO. *J. Electrochem. Soc.* **160**, F69–F74 (2013).
47. B. A. Rosen *et al.*, Ionic liquid-mediated selective conversion of CO<sub>2</sub> to CO at low overpotentials. *Science* **334**, 643–644 (2011).
48. T. N. Huan *et al.*, Porous dendritic copper: An electrocatalyst for highly selective CO<sub>2</sub> reduction to formate in water/ionic liquid electrolyte. *Chem. Sci.* **8**, 742–747 (2017).
49. E. B. Cole *et al.*, Using a one-electron shuttle for the multielectron reduction of CO<sub>2</sub> to methanol: Kinetic, mechanistic, and structural insights. *J. Am. Chem. Soc.* **132**, 11539–11551 (2010).
50. Z. Han, R. Kortlever, H. Y. Chen, J. C. Peters, T. Agapie, CO<sub>2</sub> reduction selective for C<sub>2</sub> products on polycrystalline copper with N-substituted pyridinium additives. *ACS Cent. Sci.* **3**, 853–859 (2017).
51. D. Raciti *et al.*, Low-overpotential electroreduction of carbon monoxide using copper nanowires. *ACS Catal.* **7**, 4467–4472 (2017).
52. C. W. Li, J. Ciston, M. W. Kanan, Electroreduction of carbon monoxide to liquid fuel on oxide-derived nanocrystalline copper. *Nature* **508**, 504–507 (2014).
53. S. Ma *et al.*, Electroreduction of carbon dioxide to hydrocarbons using bimetallic Cu-Pd catalysts with different mixing patterns. *J. Am. Chem. Soc.* **139**, 47–50 (2017).
54. Y. Hori, R. Takahashi, Y. Yoshinami, A. Murata, Electrochemical reduction of CO at a copper electrode. *J. Phys. Chem. B* **101**, 7075–7081 (1997).
55. E. Bertheussen *et al.*, Acetaldehyde as an intermediate in the electroreduction of carbon monoxide to ethanol on oxide-derived copper. *Angew. Chem. Int. Ed. Engl.* **55**, 1450–1454 (2016).
56. A. Garza, A. T. Bell, M. Head-Gordon, On the mechanism of CO<sub>2</sub> reduction at copper surfaces: Pathways to C<sub>2</sub> products. *ACS Catal.* **8**, 1490–1499 (2018).
57. Y. Y. Birdja, M. T. M. Koper, The importance of Cannizzaro-type reactions during electrocatalytic reduction of carbon dioxide. *J. Am. Chem. Soc.* **139**, 2030–2034 (2017).
58. E. F. Degering, T. Stoudt, Polymerization of acetaldehyde and crotonaldehyde catalyzed by aliphatic tertiary amines. *J. Polym. Sci.* **7**, 653–656 (1951).
59. R. Kortlever, I. Peters, S. Koper, M. T. M. Koper, Electrochemical CO<sub>2</sub> reduction to formic acid at low overpotential and with high faradaic efficiency on carbon-supported bimetallic Pd-Pt nanoparticles. *ACS Catal.* **5**, 3916–3923 (2015).
60. X. Nie, M. R. Esopi, M. J. Janik, A. Asthagiri, Selectivity of CO<sub>2</sub> reduction on copper electrodes: The role of the kinetics of elementary steps. *Angew. Chem.* **125**, 2519–2522 (2013).
61. R. Kortlever, J. Shen, K. J. P. Schouten, F. Calle-Vallejo, M. T. M. Koper, Catalysts and reaction pathways for the electrochemical reduction of carbon dioxide. *J. Phys. Chem. Lett.* **6**, 4073–4082 (2015).
62. S. Nitopi *et al.*, Progress and perspectives of electrochemical CO<sub>2</sub> reduction on copper in aqueous electrolyte. *Chem. Rev.* **119**, 7610–7672 (2019).
63. L. Wang *et al.*, Electrochemically converting carbon monoxide to liquid fuels by directing selectivity with electrode surface area. *Nat. Catal.* **2**, 702–708 (2019).